Hydrodynamic and Electrokinetic Properties of Decane Droplets in Aqueous Sodium Dodecyl Sulfate Solutions

Sarah A. Nespolo,[†] Michael A. Bevan,[‡] Derek Y. C. Chan,[§] Franz Grieser,[‡] and Geoffrey W. Stevens*,[†]

Particulate Fluids Processing Centre, University of Melbourne, Victoria 3010, Australia

Received March 15, 2001

Electrophoretic mobilities of sodium dodecyl sulfate (SDS)-stabilized decane droplets are converted to ζ-potentials with the aid of light scattering and SDS surface excess measurements. Static light scattering measurements of droplet size and shape in conjunction with dynamic light scattering measurements of droplet diffusion are used to determine the droplet hydrodynamic mobility coefficient. For the SDS concentrations used here between 0.01 and 1 mM SDS, the droplet's mobility coefficient is consistent with the droplet being a nondeformable, solid, spherical particle with no interfacial momentum transfer. The decane droplets display decreasing monodisperse radii with increasing bulk SDS concentration. The percent ionization of the SDS, or degree of counterion binding, is considered by comparing the charge corresponding to the measured ζ-potentials with the charge due to the SDS surface excess inferred from interfacial tension data. After the droplet hydrodynamic mobility coefficient and percent ionization of the interfacial SDS are considered, ζ-potentials for the SDS concentrations studied are found to be between −100 and −125 mV.

Introduction

In electrophoresis, an electric field is applied to a charged particle in aqueous solution, which results in a steady particle velocity, or electrophoretic mobility. Interpreting measured electrophoretic mobilities of solid particles in terms of particle surface charge, surface potential, and double-layer thickness has been the subject of extensive theoretical and experimental investigation.[1,2] Electrophoresis of immiscible oil droplets has also been studied,[1,3−9] but the problem is more complex because of the associated droplet hydrodynamics. Although the expression for the hydrodynamic mobility coefficient of a fluid droplet is well-known, its experimental measurement is difficult, and its interpretation is complicated because of the effects of adsorbed stabilizing surfactant and possible droplet deformation. The mobility coefficient of an oil droplet can be affected by transfer of momentum across the oil−water interface at the droplet surface. This mechanism reduces the oil droplet hydrodynamic mobility coefficient compared to that of a solid particle because the continuous phase fluid flow is coupled to internal droplet circulation through a zero shear stress boundary condition at the droplet surface. Droplet hydrodynamics are further complicated by the presence of stabilizing surfactant, which can be expected to interfere with the mechanism of momentum transfer.[4] Theories for droplet hydrodynamics have existed for some time,[10−12] but quantitative experimental evidence has only been obtained from sedimentation and electrokinetic studies of relatively large drops.[4] Droplet hydrodynamics inferred from electrokinetic measurements are further complicated by the presence of the applied electric field. There is at present no definitive comparison between theory and measurement of droplet hydrodynamics or electrokinetics.

Most droplet electrophoresis studies in the literature assume that the droplet behaves like a solid particle as far as its hydrodynamic properties are concerned and use the theory of Smoluchowski[13] to interpret the droplet surface potential, or ζ-potential. The Smoluchowski result is reasonable in the limit of thin double layers and low potential for solid particles, but for oil droplet studies it may not be valid to assume solid particle hydrodynamics without support from independent measurements.[1,4−9] Several oil droplet electrophoresis studies[14−16] have used the O'Brien and White (OW) theory,[17] but have avoided the issue of droplet hydrodynamics. To interpret the electrophoretic mobilities of oil droplets, we use the theory of Ohshima et al.,[5] which extends the OW model to include hydrodynamic effects. Baygents and Saville[7] also extended the OW theory for the analysis of bubbles and droplets to include effects due to the transport of interfacial species,

* To whom correspondence should be addressed. E-mail: gstevens@unimelb.edu.au.
[†] Department of Chemical Engineering.
[‡] School of Chemistry.
[§] Department of Mathematics and Statistics.

(1) Hunter, R. J. *Zeta Potential in Colloid Science*; Academic Press Inc.: London, 1981.
(2) Russel, W. B.; Saville, D. A.; Schowalter, W. R. *Colloidal Dispersions*; Cambridge University Press: Cambridge, U.K., 1989.
(3) Booth, F. *J. Chem. Phys* **1951**, *19*, 1331.
(4) Levich, V. G. *Physicochemical Hydrodynamics*; Prentice Hall: Upper Saddle River, NJ, 1962.
(5) Ohshima, H.; Healy, T. W.; White, L. R. *J. Chem. Soc., Faraday Trans. 2* **1984**, *80*, 1643.
(6) Levine, S.; O'Brien, R. N. *J. Colloid Interface Sci.* **1973**, *43*, 616.
(7) Baygents, J. C.; Saville, D. A. *J. Chem. Soc., Faraday Trans.* **1991**, *87*, 1883.
(8) Baygents, J. C.; Saville, D. A. *J. Colloid Interface Sci.* **1991**, *146*, 9.
(9) Ohshima, H. *J. Colloid Interface Sci.* **1997**, *189*, 376.
(10) Hadamard, J. S. *C. R. Acad. Sci.* **1911**, *152*, 1735.
(11) Rybczynski, W. *Bull. Acad. Sci. Cracovie* **1911**, *A*, 40.
(12) Boussinesq, M. J. *Math. Pure Appl.* **1905**, *6*, 285.
(13) Smoluchowski, M. *Z. Phys. Chem.* **1918**, *93*, 129.
(14) Barchini, R.; Saville, D. A. *Langmuir* **1996**, *12*, 1442.
(15) Dunstan, D. E.; Saville, D. A. *J. Chem. Soc., Faraday Trans.* **1992**, *88*, 2031.
(16) Dunstan, D. E. *J. Colloid Interface Sci.* **1994**, *166*, 472.
(17) O'Brien, R.; White, L. R. *J Chem Soc., Faraday Trans. 2* **1978**, *74*, 1607.

10.1021/la0103968 CCC: $20.00
Published on Web 10/20/2001

but the data presented in this paper do not warrant modeling at this level of detail.

In the present study, we measure electrophoretic mobilities of sodium dodecyl sulfate (SDS)/decane droplets with varying SDS concentration below the critical micelle concentration (CMC). We also measure the oil droplet hydrodynamic mobility coefficient and SDS interfacial excess for the same SDS concentrations used in the electrokinetic studies. Depending on whether one assumes the droplet behaves hydrodynamically as a solid particle or as a liquid particle, each measured electrophoretic mobility value can allow up to four possible corresponding ζ-potentials, as opposed to at most two solutions for solid particles. It is therefore necessary to acquire additional experimental information to obtain a unique ζ-potential for each experimentally measured electrophoretic mobility.

To determine the droplet hydrodynamic mobility coefficient, static light scattering is used to measure droplet shape and size, and dynamic light scattering is used to measure droplet diffusion, from which the hydrodynamic mobility coefficient is determined. With measurement of these independent parameters, the effect of internal droplet flow on the droplet hydrodynamic mobility coefficient can be determined uniquely. Although several studies have probed concentrated emulsions using static and dynamic light scattering,[18−20] no previous study has attempted to measure the droplet hydrodynamic mobility coefficient using these combined techniques. After the hydrodynamic properties of the SDS/decane droplets are considered, several ζ-potential choices remain possible when the measured droplet electrophoretic mobilities are interpreted. Additional measurements of interfacial tension are then used to compare the ζ-potential, droplet surface charge, and amount of adsorbed surfactant. These data allow the correct ζ-potentials to be chosen which correspond to reasonable values of the degree of ionization, or the degree of counterion binding, of sodium ions with surfactant molecules at the droplet surface. When all of these data together are considered together, it is possible to pick a unique ζ-potential at each SDS concentration studied.

Theory

Static and Dynamic Light Scattering. Light scattering experiments measure the intensity of light scattered from a sample at a given angle relative to the incident beam. The angle at which the light scattering is observed, θ, determines the length scale in light scattering experiments, or the magnitude of the scattering wave vector, q, as

$$q = \frac{4\pi n}{\lambda}\sin\left(\frac{\theta}{2}\right) \tag{1}$$

where n is the refractive index of the continuous medium and λ is the vacuum wavelength of the incident light. In static light-scattering (SLS) experiments, the time-averaged excess scattering intensity, $\Delta I(q)$, is measured as a function of the wave vector, q, and is given most generally by[21]

$$\Delta I(q) = I(q) - I_b(q) \cong K_1 P(q,a)\, S(q) \tag{2}$$

where $I(q)$ is the total scattering intensity, $I_b(q)$ is the scattering from the solvent, background, and photometry noise, and K_1 is a proportionality constant depending on instrumental parameters and particle concentration. The form factor, $P(q,a)$, depends on particle shape and size, and the structure factor, $S(q)$, depends on particle interactions. For a dilute dispersion of particles in which interparticle colloidal forces are unimportant, $S(q)$ tends to unity and its contribution to eq 2 may be ignored. For a dispersion of spheres of radius a, $P(q,a)$ is given as[22]

$$P(q,a) = \left[\frac{3(\sin(aq) - aq\cos(aq))}{(aq)^3}\right]^2 \tag{3}$$

By combining eqs 2 and 3, it is possible to obtain the radius of monodisperse spheres in a dilute dispersion by plotting $\Delta I(q)$ as a function of q and fitting for K_1 and a. This result is due to Rayleigh and is applicable to particles of size a, provided[22]

$$|m - 1| \ll 1 \quad \text{and} \quad \frac{4\pi a}{\lambda}|m - 1| \ll 1 \tag{4}$$

where $m = n_1/n_2$ is the refractive index ratio, with n_1 equal to the particle refractive index and n_2 equal to the medium refractive index.

In dynamic light scattering (DLS) experiments, the time dependence of the light scattering intensity is measured at a particular scattering angle, θ, or wave vector, q. The time dependence of the scattered intensity is measured in DLS by the intensity autocorrelation function, $g^{(2)}(\tau)$, which can be interpreted as an average self-diffusion coefficient via the following expression:[23]

$$g^{(2)}(\tau) = \frac{\langle I(0)\, I(0+\tau)\rangle}{\langle I(0)\rangle^2} = 1 + K_2 \exp(-2Dq^2\tau) \tag{5}$$

where τ is the delay time, K_2 is an instrumental constant, and D is the average self-diffusion coefficient. The diffusion coefficient, D, and the constant, K_2, are obtained by fitting eq 5 to the intensity autocorrelation function as a function of delay time.

Droplet Diffusion and Mobility. The diffusion coefficient, D, and hydrodynamic mobility coefficient, α, of a single spherical particle for infinitely dilute conditions are related via the Stokes−Einstein equation

$$D = kT/\alpha \tag{6}$$

where k is Boltzmann's constant and T is absolute temperature. The hydrodynamic mobility coefficient, α, of an uncharged solid sphere of radius a for Stokes flow in an unbounded fluid is

$$\alpha = 6\pi\eta a \tag{7}$$

where η is the fluid medium viscosity. Using eqs 5−7, the radius of an uncharged spherical solid particle can be determined using DLS. The more general result for the mobility coefficient of any spherical droplet with a continuity of shear stress hydrodynamic boundary condi-

(18) Cheung, H. M.; Qutubuddin, S.; Edwards, R. V.; Mann, J. A., Jr. *Langmuir* **1987**, *3*, 744.
(19) Chang, N. J.; Kaler, E. W. *Langmuir* **1986**, *2*, 184.
(20) Guest, D.; Langevin, D. *J. Colloid Interface Sci.* **1986**, *112*, 208.
(21) Kerker, M. *The Scattering of Light and Other Electromagnetic Radiation*; Academic Press Inc.: New York, 1969.
(22) van de Hulst, H. C. *Light Scattering by Small Particles*; John Wiley & Sons: New York, 1957.
(23) Berne, B. J.; Pecora, R. *Dynamic Light Scattering with Applications to Chemistry, Biology, and Physics*; John Wiley & Sons: New York, 1976.

tion at the droplet surface is[24]

$$\alpha(\lambda) = f(\lambda)6\pi\eta_o a \tag{8}$$

where

$$f(\lambda) = \frac{^2/_3 + \lambda}{1 + \lambda} \quad \text{and} \quad \lambda = \frac{\eta_i}{\eta_o} \tag{9}$$

and η_i is the viscosity of the fluid inside the droplet and η_o is the viscosity of fluid outside the droplet, or the continuous medium viscosity. Some useful limits to consider for this expression are for the cases of an infinite droplet viscosity ($\lambda \rightarrow \infty$), which reduces to a solid particle, and an inviscid fluid droplet ($\lambda \rightarrow 0$), such as an air bubble:

$$\lim_{\lambda\to\infty} \alpha(\lambda) = 6\pi\eta_o a \quad \text{and} \quad \lim_{\lambda\to 0} \alpha(\lambda) = 4\pi\eta_o a \tag{10}$$

For a charged particle moving through a fluid, ions associated with the electrical double layer distort the local flow field of the surrounding fluid. As a result, the potential at the plane of shear on the droplet surface, or the ζ-potential, and the scaled thickness of the double layer, κa, are important in determining additional dissipative effects, and eq 8 is generalized to

$$\alpha(\lambda,\zeta,\kappa a) = f(\lambda,\zeta,\kappa a)6\pi\eta_o a \tag{11}$$

where $f(\lambda,\zeta,\kappa a)$ can be evaluated using electrokinetic theory[17] and κ is the inverse of the Debye length. It is possible to determine experimentally the collective terms $6f(\lambda,\zeta,\kappa a)$ by combining eqs 6 and 11 and using the SLS measured droplet radius, a_{sls}, and the DLS measured diffusion coefficient, D_{dls}, to give

$$6f(\lambda,\zeta,\kappa a) = \frac{\alpha(\lambda,\zeta,\kappa a)}{\pi\eta_o a_{sls}} = \frac{kT}{\pi\eta_o a_{sls} D_{dls}} \tag{12}$$

where the middle part of eq 12 is a rearrangement of eq 11 and the right-hand side is a rearrangement of eq 6.

Electrophoretic Mobility of Droplets. For a charged particle, the velocity, U, at which it moves in the presence of a weak electric field is linearly related to the strength of the applied field, E, by

$$U = \mu E \tag{13}$$

where the factor μ is commonly referred to as the electrophoretic mobility. The solution for μ in eq 13 is obtained by balancing the force required to move a charged particle at velocity U in a stagnant fluid with no applied electric field and the force required to hold a charged particle stationary in an applied field of strength E.[17] This force balance can be written as

$$\sum F = \alpha U + \beta E = 0 \tag{14}$$

where the coefficients α and β are independent of U and E for weak fields. The mobility coefficient, α, can be obtained experimentally for a charged oil droplet using eq 12, while the coefficient β must be computed from theory.[5,17] For a charged oil droplet in water, the electrophoretic mobility, μ, determined experimentally, can be related to the ζ-potential by combining eqs 13 and 14 to obtain[5]

$$\mu = \frac{U}{E} = -\frac{\beta(\lambda,\zeta,\kappa a)}{\alpha(\lambda,\zeta,\kappa a)} \tag{15}$$

so that ζ can be obtained numerically from eq 15.[5]

Interfacial Charge, Surface Tension, and Surfactant Surface Excess. Using the Gouy−Chapman model of the electrical double layer, it is possible to relate the surface potential, ψ, and surface charge density, σ, of a charged interface. The surface potential, ψ, is defined to occur at the rigid particle surface, and is not necessarily the same as the electrokinetically relevant ζ-potential, which occurs at the plane of shear next to the charged interface. For the purpose of this study, as will be discussed, it is adequate to assume that $\psi \approx \zeta$ so that the relationship between σ and ζ-potential for a 1:1 electrolyte can be interpreted as[2]

$$\sigma_\zeta = \frac{2kT\epsilon_0\epsilon_w\kappa}{e}\sinh\left[\frac{e\zeta}{2kT}\right] \tag{16}$$

where ϵ_0 is the vacuum permittivity, ϵ_w is the permittivity of water, and e is the magnitude of charge on a single electron. This equation provides one estimate of the surface charge density on the droplet.

A second, and independent, estimate of the surface charge on the droplet can be obtained from the adsorption density of surfactant molecules at the oil droplet surface and the degree of counterion binding. Using the Gibbs equation,[25] the surface excess of surfactant at the oil−water interface, Γ, can be determined from interfacial tension data as a function of bulk surfactant concentration. The surface excess of a 1:1 surfactant (XS) in the presence of a constant concentration of 1:1 electrolyte (XA), which shares the same cation (X^+) as the surfactant, is given by[26]

$$\Gamma = -\frac{1}{N_A kT}\left[\frac{C_{XA}/C_{XS} + 0.5}{C_{XA}/C_{XS} + 1}\right]\left[\frac{d\gamma}{d\ln C_{XS}}\right]_{C_{XA}} \tag{17}$$

where γ is the interfacial tension of the droplet oil−water interface, N_A is Avogadro's number, C_{XS} is the bulk concentration of a 1:1 surfactant in the aqueous medium, and C_{XA} is the bulk concentration of a 1:1 electrolyte which shares the same cation (X^+) as the surfactant. This result assumes that the 1:1 electrolyte anion (A^-) does not significantly affect interfacial tension or adsorb at the oil−water interface, and that both components are dilute enough to use concentration rather than activity in eq 17. For the cases of zero electrolyte concentration and electrolyte concentration much greater than the surfactant concentration, the two commonly recognized limits, respectively, are

$$\lim_{C_{XA}/C_{XS}\to 0} \Gamma = -\frac{1}{2N_A kT}\left[\frac{d\gamma}{d\ln C_{XS}}\right] \tag{18a}$$

and

$$\lim_{C_{XA}/C_{XS}\to \infty} \Gamma = -\frac{1}{N_A kT}\left[\frac{d\gamma}{d\ln C_{XS}}\right] \tag{18b}$$

The surface charge density corresponding to complete surfactant ionization can be determined by expressing the surface excess as a number area density and multiplying by the unit charge:

(24) Happel, J.; Brenner, H. *Low Reynolds number hydrodynamics*; Prentice Hall: Upper Saddle River, NJ, 1965.

(25) Adamson, A. W. *Physical Chemistry of Surfaces*; John Wiley & Sons: New York, 1997.

(26) Tajima, K. *Bull. Chem. Soc. Jpn.* **1971**, *44*, 1767.

$$\sigma_\Gamma = e\Gamma \tag{19}$$

Experimental Details

Materials. Polystyrene (PS) surfactant-free latex spheres with sulfate groups and a nominal average diameter of 0.2 μm were obtained from Interfacial Dynamics Corp. (batch no. 758, product no. 1-200) and used without further cleaning. Larger PS spheres with a nominal diameter of 360 nm were prepared with a surfactant-free emulsion polymerization method.[27] The anionic SDS was obtained from BDH Laboratory Supplies. Sample purity was verified by using solution conductivity to measure the CMC as 7.9 mM, which is in good agreement with literature measurements.[28]

The aqueous SDS/decane emulsions were prepared by rapidly injecting decane into a background solution of 0.1 M SDS and 1 mM $NaNO_3$ to give a droplet volume fraction of $\sim 10^{-5}$. This mixture was shaken and then sonicated for 1 h. The desired background SDS concentration was obtained by further dilution with 1 mM $NaNO_3$ followed by additional shaking and sonication. These solutions were allowed to stand overnight prior to light scattering or electrophoresis measurements the next day.

All samples were prepared using double-deionized water. All glassware was cleaned by soaking in 10% nitric acid and then by sonication for 1 h in a 1% RBS detergent (Pierce Chemicals)/20% ethanol solution, followed by extensive rinsing with double-deionized water.

Methods. For measurements of electrophoretic mobilities, a Coulter DELSA 440 laser Doppler apparatus was used. The incident wavelength was 633.0 nm, and the applied voltage for the reported data was 5.00 V. Control studies of SDS/decane electrophoretic mobilities at 2.00, 5.00, 10.0, and 20.0 V/cm indicated a linear response with electric field magnitude. Measurements were made at the stationary layers, with reported values being the average of the two that were in agreement within 10%. The conductivity and temperature were constant during each measurement, indicating minimal joule heating. A constant temperature of 25.0 ± 0.1 °C was maintained using instrument temperature control. The reported mobilities are averages of 10 measurements for each sample.

For light scattering measurements a Malvern 4700 apparatus with an Ar^+ ion laser was used. All measurements were performed at a temperature of 25.0 ± 0.1 °C maintained with an ethanol bath. PS particle samples were prepared by filling the scattering cell with ~2.5 mL of 10^{-2} M NaCl followed by ~0.5 mL of dispersion. The cell was then emptied, and the wall residue was diluted with ~3 mL of 10^{-2} M NaCl to achieve a final sample concentration of $\sim 10^{-6}$ volume fraction. The 10^{-2} M NaCl was used to suppress electroviscous effects, while maintaining dispersion stability. Droplet samples were prepared at low volume fractions suitable for light scattering experiments so that further dilution was not required. The photomultiplier tube aperture was adjusted in each experiment to maintain $\sim 3 \times 10^6$ counts/s. SLS measurements were performed at 20 angles between 30° and 140° with typical measurement times of 100 s at each angle. DLS measurements were each performed at several angles using delay times and total scan times optimized with the aid of instrument software.

Interfacial tension data were obtained using an FTÅ200 pendant droplet instrument. All measurements were performed at a temperature of 25.0 ± 0.1 °C using a water bath. Images were obtained at 2 frames/s for a period of 30 s.

Results and Discussion

Interpretation of ζ-Potential from Electrophoretic Mobilities of Aqueous SDS/Decane Droplets. In Table 1 electrophoretic mobilities, μ, are listed for decane droplets in 1 mM $NaNO_3$ and 0.01, 0.1, and 1 mM bulk SDS solutions. The reported μ values are the average of 10 mobility measurements at each SDS concentration. The values of κa also listed in Table 1 were calculated using the $NaNO_3$ and SDS concentrations. The κa values, which are important parameters for the electrokinetic calculations, were determined using the droplet radii measured with static light scattering. Interpreting μ with standard electrokinetic theories requires that the droplets behave as nondeformable spheres in an applied electric field. The nondeformable, spherical nature of the droplets is suggested by the measured linear response of μ with varying strength of the electric field and is confirmed by static light scattering data in the following section. The linear response of μ with respect to field strength also suggests that Marangoni effects due to interfacial surfactant concentration gradients are unimportant, although this cannot be directly probed in this experiment. Additionally, conversion of μ to ζ-potential requires assuming the SDS/decane droplets behave hydrodynamically as either solid particles or liquid droplets. In Figure 1 we show the relationship between ζ-potential and μ for both solid particles and liquid droplets using the theories of O'Brien and White[17] and Ohshima et al.[5] It is clear that for a given μ there can be up to four possible ζ-potential values depending on the droplet hydrodynamics. For the μ values listed in Table 1, the possible corresponding ζ-potentials are given in Table 2.

In Figure 1 the 1 mM SDS/decane droplet mobility value reported in Table 1 is shown by the horizontal solid line. The gray region surrounding the line indicates the error range determined from the distribution of 10 measured mobilities. For the liquid or solid models of the droplet, the corresponding possible ζ-potentials are indicated by

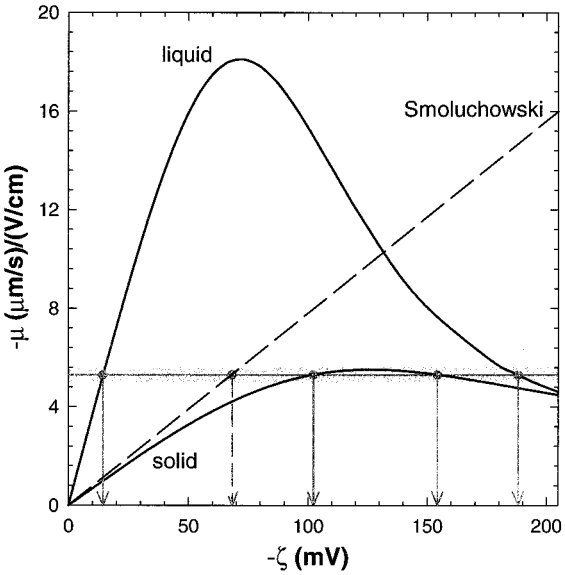

Figure 1. Mobility as a function of ζ-potential calculated for both solid and liquid particles in 1 mM SDS/1 mM $NaNO_3$ with $\kappa a = 20.38$ using the standard theory.[5,17] The viscosity of decane is 0.92 cP at 298 K. The horizontal solid gray line is the measured mobility of 5.3 (μm/s)/(V/cm). The vertical solid gray lines indicate ζ-potential for both the liquid (−14 and −188 mV) and solid particles (−103 and −154 mV). The Smoluchowski equation relating μ and ζ is given as the broken straight line. The shaded area indicates error ranges of the experimental mobility value.

Table 1. Electrophoretic Measurements of Decane Droplets in Aqueous SDS Solutions and 10^{-3} M $NaNO_3$ at 298 K

[SDS]	1×10^{-3} M	1×10^{-4} M	1×10^{-5} M
μ [(μm/s)(V/cm)]	5.30 ± 0.27	5.65 ± 0.20	5.70 ± 0.20
κa_{sls}	20.4	21.2	28.5

(27) Goodwin, J. W.; Hearn, J.; Ho, C. C.; Ottewill, R. H. *Colloid Polym. Sci.* **1974**, *252*, 464.

(28) Rosen, M. J. *Surfactants and Interfacial Phenomena*; John Wiley & Sons: New York, 1974.

Table 2. Magnitude of the ζ-Potential Ranges (mV) from Electrophoretic Mobility (μ), Light Scattering (LS), and Surface Excess (Γ) Experiments at 298 K

		|ζ|-potential (mV)		
		1×10^{-3} M SDS	1×10^{-4} M SDS	1×10^{-5} M SDS
μ	liquid 1	13−14	13−14	11
	liquid 2	182−194	179−187	190−194
	solid 1	90−127	108−148	94−112
	solid 2	127−173		154−176
μ, LS	liquid 2	182−194	179−187	190−194
	solid 1	90−127	108−148	94−112
	solid 2	127−173		154−176
μ, LS, Γ	solid 1	90−127	108−148	94−112

vertical arrows. The uncertainties in the estimated ζ-potentials were also determined from the error range (the gray area) of the measured mobility. For the 1 mM SDS/decane case, Figure 1 indicates that the measured mobility of -5.30 ± 0.27 (μm·cm)/(V·s) corresponds to four possible ζ-potentials including −14, −109, −154, and −188 mV. Also it can be seen from Figure 1, for the case of a solid particle, a small error in the mobility leads to a particularly large uncertainty for ζ-potentials between −90 and −173 mV. The uncertainty in ζ-potentials is particularly large in this case because of the proximity of the measured mobility to the maximum in the solid particle mobility curve. For reference, the Smoluchowski prediction for a solid particle is indicated by the dashed line, which gives $\zeta = -68$ mV. The same analysis was performed for each SDS concentration to determine possible ζ-potentials, with the results reported in Table 2 for each case. Since each of the measured mobilities in Table 1 can correspond to four possible ζ-potentials, additional information is required to determine the unique ζ-potential in each case.

Part of the difficulty with converting the measured μ values to ζ-potentials is knowing whether to model the oil droplet as a liquid droplet or a solid particle. The hydrodynamic mobility coefficient, α, for a liquid droplet moving though a fluid can be considerably less than that for a solid particle because of the ability for momentum to be transferred across the droplet's oil−water interface into the interior of the oil droplet, which produces internal flow or circulation. It is not obvious how surfactant molecules adsorbing to the droplet surface interfere with momentum transfer at the oil−water interface, although they are expected to retard rather than enhance surface flow. While oil droplet hydrodynamics, and electrophoresis in particular, have been the subject of extensive theoretical modeling,[1,4−9] experimental measurements have generally ignored the problem of internal flows and treat droplets as hard particles. This is perhaps due to the nontrivial task of measuring the degree of momentum transfer at the oil−water interface of a submicrometer oil droplet.

In addition to the effects of internal flow, the oil droplet hydrodynamic mobility coefficient, α, is further complicated by an additional dissipative mechanism due to droplet surface charge, which is essentially the "primary electroviscous effect".[1] Fluid flow near any charged particle surface experiences an "electroviscous" drag because of the tendency for the spatial ion distribution associated with the surface charge, or electrical double layer, to resist distortion in the flow field. The predicted magnitude of this effect on the liquid droplet mobility coefficient is shown in Figure 2 for the nondimensional hydrodynamic mobility coefficient, $\alpha/(\pi\eta a)$, as a function of ζ-potential for the solid particle and liquid droplet cases corresponding to Figure 1. The four possible ζ-potentials shown in Figure 1 are also indicated by vertical arrows in Figure 2. For the

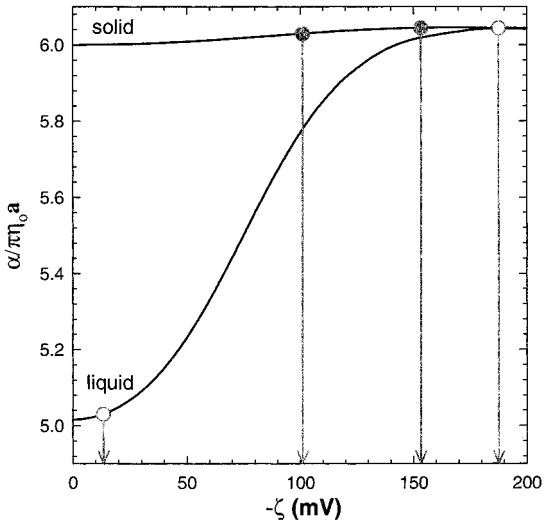

Figure 2. Theoretical prediction[5,17] of the nondimensional mobility coefficient as a function of ζ-potential for the solid (●) and liquid (○) cases as used for the predictions in Figure 1.

solid particle model with $\alpha/(\pi\eta a) = 6$ for $\zeta = 0$, $\alpha/(\pi\eta a)$ rises gradually to ∼6.02 in the limit of high potential. For the liquid droplet model, $\alpha/(\pi\eta a)$ initially starts at the decane/water limit around $\alpha/(\pi\eta a) = 5$ for $\zeta = 0$ and then increases to ∼6.02 for high potentials. This indicates that electroviscous effects dominate the hydrodynamic mobility coefficient in the high ζ-potential limit and mask effects due to internal droplet flow. As a result of the dominant electroviscous contribution for droplets in the high potential limit, the liquid droplet and the solid particle solutions converge to the same value of α. The three highest ζ-potentials in Figures 1 and 2 all have $\alpha/(\pi\eta a) \approx 6$ even though the highest potential corresponds to the liquid droplet case. In the limit of high surface potential, internal droplet flow does not play an obvious role when μ is interpreted, at least in terms of the effects on α.

A direct experimental determination of the droplet hydrodynamic mobility coefficient, α, is necessary to convert the electrophoretic mobility, μ, to ζ-potential.[1,7] Although past droplet sedimentation studies have interpreted a solid particle α for millimeter-sized droplets,[4] none of these investigations have directly measured α for low Peclet and Reynolds number submicrometer droplets. It is also possible that the α inferred in some of these past studies may suffer from misinterpretation since they predate the now standard electrokinetic theories of O'Brien and White[17] and Ohshima et al.[5] To our knowledge, no study has performed self-consistent measurements of both droplet motion, whether diffusion or migration in a force field, and droplet size and shape. It is necessary to measure droplet motion and shape independently to determine the droplet α, which can be achieved using static and dynamic light scattering.

Interpretation of ζ-Potentials from Static and Dynamic Light Scattering. To interpret the oil droplet α using light scattering, it is necessary to recall that the droplet diffusion coefficient, *D*, is inversely proportional to α with *kT* as the coefficient in the Stokes−Einstein equation, eq 7. By measuring the diffusion coefficient of oil droplets in the submicrometer range using DLS, α can then be obtained using the Stokes−Einstein equation, but additional information is required to interpret this measured α in terms of the physical properties of the droplet. Determining the degree of momentum transfer at the droplet surface requires independent knowledge of the droplet size and shape to interpret the hydrodynamics.

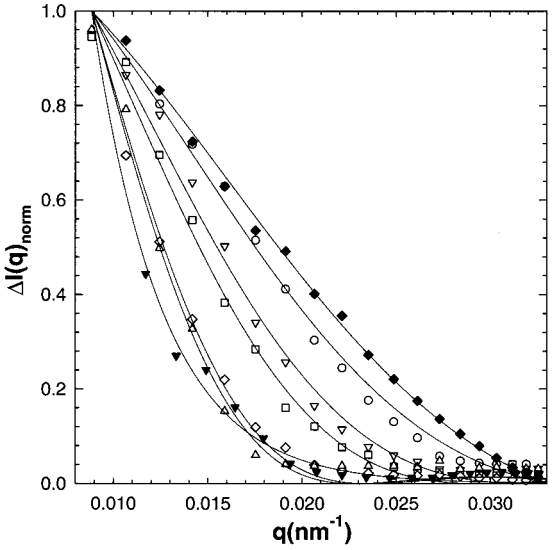

Figure 3. Angular dependence of the scaled excess scattering intensity for IDC latex (◆), synthesized latex (▼), and decane droplets in SDS concentrations of (○) 5 mM, (▽) 1 mM, (□) 0.5 mM, (◇) 0.1 mM, and (△) 0.01 mM. The fits of the form factor, $P(q)$ (eq 3), are given by the solid lines.

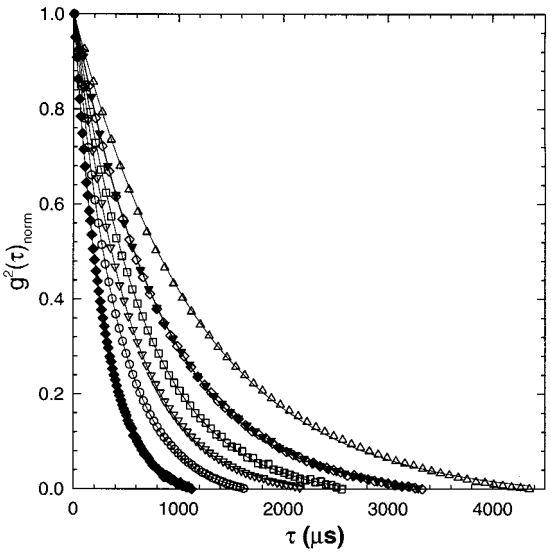

Figure 4. Normalized intensity autocorrelation function at a scattering angle of 90° for IDC latex (◆), synthesized latex (▼), and decane droplets in SDS concentrations of (○) 5 mM, (▽) 1 mM, (□) 0.5 mM, (◇) 0.1 mM, and (△) 0.01 mM. The fits of the normalized intensity autocorrelation function, $g^{(2)}(\tau)$ (eq 5), are given by the solid lines.

By using SLS, the oil droplet size and shape can be determined independently of D, and effects due to momentum transfer at the interface can then be estimated using eq 12. The combination of DLS and SLS experiments also has the benefit of using the same sample in both experiments, which provides internal checks for self-consistency between the two analyses. In addition to determining α, the SLS measurements are also important for confirming the droplets' spherical shape and determining κa, which are important parameters in the theoretical predictions in Figure 1.

In Figure 3 we show the results of SLS experiments for SDS/decane droplets and PS particles. Two PS particle sizes were used for calibration and for comparison with the droplet data, since previous SLS/DLS studies of PS particles have been shown to produce the quantitative self-consistent results expected for solid, monodisperse spheres.[29] The SLS data in Figure 3 show the normalized excess scattering intensity, ΔI, for a range of q which corresponds to angles between 30° and 140°. The DLS data in Figure 4 show the normalized intensity autocorrelation function, $g^{(2)}(\tau)_{\text{norm}}$, as a function of the correlator delay time, τ, measured at a scattering angle of 90°. Figure 4 shows DLS data for one scattering angle to display the trend for all of the results. All DLS measurements were performed at several angles to ensure measurement of single-particle diffusion, or to ensure no contributions to the total scattering intensity from particle interactions via $S(q)$ in eq 2. In Figures 3 and 4 the open symbols refer to the SDS/decane data and the filled symbols to the PS particle data. To display all of the data in Figures 3 and 4, the data and curve fits were normalized using

$$\Delta I(q)_{\text{norm}} = \frac{I(q) - I_{\text{min}}}{I_{\text{fit}}(0.008\ \text{nm}^{-1}) - I_{\text{min}}} \qquad (20a)$$

and

$$g^{(2)}(\tau)_{\text{norm}} = \frac{g^{(2)}(\tau) - g(\tau)_{\text{min}}}{g(0) - g(\tau)_{\text{min}}} \qquad (20b)$$

where I_{min} and $g(T)_{\text{min}}$ are the minimum detectable values.

Table 3. Summary of Light Scattering Experiments at 298 K for PS and SDS Stabilized Decane Droplets

	type	a_{sls} (nm), 100% ΔI	a_{sls} (nm), 85% ΔI	D_{dls} (cm²/s)	$\alpha/\pi\eta a$
PS latex	IDC	105.3 ± 1.9	105.1 ± 1.9	2.34 ± 0.14	5.97 ± 0.45
	EP	179.0 ± 6.1	178.0 ± 6.0	1.28 ± 0.05	6.42 ± 0.47
	SDS (M)	a_{sls} (nm), 100% ΔI	a_{sls} (nm), 85% ΔI	D_{dls} (cm²/s)	$\alpha/\pi\eta a$
decane	5×10^{-3}	113.5 ± 2.7	113.0 ± 2.5	2.11 ± 0.06	6.14 ± 0.33
	1×10^{-3}	138.6 ± 2.5	138.3 ± 2.3	1.69 ± 0.2	6.28 ± 0.24
	5×10^{-4}	156.7 ± 7.7	154.2 ± 7.0	1.57 ± 0.02	5.96 ± 0.38
	1×10^{-4}	194.6 ± 5.1	187.8 ± 5.0	1.26 ± 0.11	6.00 ± 0.67
	1×10^{-5}	203.7 ± 5.5	196.8 ± 5.1	0.90 ± 0.05	≫6

The fitted curves in Figures 3 and 4 use eq 2 in combination with eqs 3 and 5 for the SLS and DLS data, respectively. The results of the SLS and DLS fits are reported in Table 3 as droplet radius, a_{sls}, from eq 3 and droplet diffusion coefficient, D_{dls}, from eq 5. Two columns in Table 3 list a_{sls} values, which were obtained by fitting either the entire curve for each data set shown in Figure 3 or the upper 85% of intensities. This was done to estimate the effect of noise in each fit, which appears to be minimal since there is no appreciable difference between the radii given by the two fits. Table 3 also includes the nondimensional mobility coefficient, $\alpha/(\pi\eta a)$, calculated from eq 12, which indicates the combined effects of momentum transfer and electroviscous effects on α. Although electroviscous effects were minimized by working at a reasonably high κa, the effect of the ζ-potential on α could not be removed.

In Table 3 the experimental nondimensional mobility coefficient, $\alpha/(\pi\eta a)$, is close to 6 in all cases, consistent with a solid particle α, except for the 0.01 mM SDS/decane droplet case, which has $\alpha > 6$. The α for the 0.01 mM SDS/decane case appears to be in error since the measured α must be between 4 and ~6.02. If D_{dls} is assumed to be correct for the 0.01 mM SDS case, a_{sls} would have to be greater than 270 nm to produce an α corresponding to liquid droplet hydrodynamics, or $\alpha/(\pi\eta a) \leq 6$. This would require the measured $a_{\text{sls}} = 200$ nm to be in error by greater

(29) Min, G.; Bevan, M.; Prieve, D. C.; Patterson, G. D. *Colloids Surf., A*, submitted for publication.

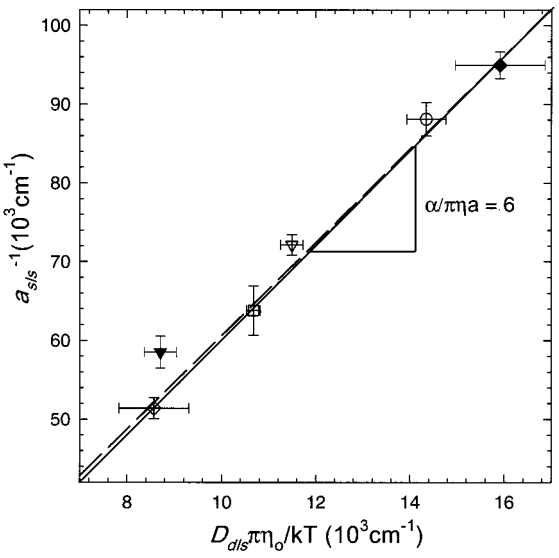

Figure 5. Inverse of the radius obtained from SLS measurements, (a_{sls}^{-1}), as a function of the quantity $D\pi\mu/kT$, with the diffusion coefficient, D, obtained from DLS measurements: IDC latex (◆), synthesized latex (▼), and decane droplets in SDS concentrations of (○) 5 mM, (▽) 1 mM, (□) 0.5 mM, and (◇) 0.1 mM. The fitted line (---) for the SDS/decane droplets gives $\alpha = 6.12$, and the reference line (—) is for $\alpha = 6$ as given by eq 12.

than 35%. The possibility that Rayleigh theory is inapplicable for analyzing the 0.01 mM SDS/decane system was considered. The larger PS particle with $(4\pi a/\lambda)|m - 1| = 0.9$ is less satisfactory with respect to the limits of Rayleigh scattering than the 0.01 mM SDS/decane droplet with $(4\pi a/\lambda)|m - 1| = 0.4$, but the larger PS particle has $\alpha/(\pi\eta a) = 6$ within experimental error. This suggests that the Rayleigh theory should be adequate for the SDS/decane droplet, although admittedly a source of some error. It is more likely that the error in the 0.01 mM SDS/decane case is due to a low absolute scattering intensity as a result of the small decane volume fraction dispersed. Low scattering intensities would cause signal noise to produce significant distortion of the SLS data and curve fit, particularly at small q. This type of noise is less of a factor for determining D_{dls}, which is determined from the time dependence of the intensity signal at a given value of q. This is consistent with the initial assumption that D_{dls} is reasonably accurate in this measurement. Although the inequality $\alpha/(\pi\eta a) < 6$ is most likely to hold for the 0.01 mM SDS case because it has the least interfacial surfactant to interfere with momentum transfer, the measured $\alpha/(\pi\eta a)$ turned out to be much greater than 6. An error is excess of 35% in a_{sls} that would be necessary to make $\alpha/(\pi\eta a) < 6$, or produce liquid droplet hydrodynamics, is unlikely in these experiments, so the 0.01 mM SDS case also most likely corresponds to $\alpha = 6$. It seems reasonable to conclude that the experimental $\alpha/(\pi\eta a)$ values reported in Table 3 all correspond to solid particle hydrodynamic mobility coefficients.

The light scattering data, excluding the 0.01 mM SDS/decane case, are also summarized in Figure 5 in addition to the results reported in Table 3. In Figure 5 a_{sls}^{-1} is shown as a function of $D_{dls}\pi\eta/kT$ for solid particles and droplets with an average $\alpha/(\pi\eta a) = 6.12$ from the regressed slope. The data point for the synthesized 360 nm PS particles is furthest from the $\alpha/(\pi\eta a) = 6$ line probably because of the Rayleigh scattering issues already discussed ($(4\pi a/\lambda)|m - 1| = 0.9$ for the 360 nm PS particle). All of the SDS/decane SLS and DLS data shown in Table 3 and Figure 5 are consistent with the droplets behaving as nondeformable, solid, monodisperse spheres. Although some degree of polydispersity in the droplet size is certainly present, the quality of the curve fits in Figures 3 and 4 using the monodisperse sphere form factor in eq 3 are adequate for quantitative analysis of the droplet α. The oil droplet radii are also observed to decrease with increasing SDS concentration, which is consistent with a reduction in the droplet interfacial tension, or Laplace pressure; however, the oil volume fraction was not controlled to allow for quantitative examination of this trend. It should also be noted that droplet shape fluctuations were not evident within the DLS temporal or SLS spatial resolutions, and are probably unimportant for interpreting droplet electrophoresis. The DLS and SLS data reported in Table 3 and Figure 5 are consistent with the droplets being nondeformable, solid, monodisperse spheres with no internal flow, which give $\alpha/(\pi\eta a) = 6$ within experimental error for both the SDS/decane droplets and PS particles.

It is now possible to further interpret the electrophoretic mobilities, μ, reported in Table 1 using $\alpha/(\pi\eta a) = 6$. Returning to Figures 1 and 2 in the example case, it can now be seen that $\zeta = -14$ mV can be rejected, because this requires $\alpha/(\pi\eta a) = 5$. However, the other three ζ-potential options all have $\alpha/(\pi\eta a) = 6$ and therefore remain reasonable choices. The high ζ-potential liquid droplet case has $\alpha/(\pi\eta a) = 6$ due to dominant electroviscous effects, so the light scattering results cannot be used to rule out this possible solution. The second row of Table 2 now indicates a reduced number of possible ζ-potentials, and required assumptions, for interpreting the experimental μ. To make further progress in interpreting μ, it is relevant to consider SDS surface excess data obtained from interfacial tension measurements. Although the light scattering data provide information concerning droplet hydrodynamics relevant to electrophoresis, the SDS surface excess can be used to understand the possible ζ-potentials in terms of interfacial surfactant counterion binding.

Interpretation of ζ-Potentials from Interfacial Tension Data (SDS Surface Excess). The electrophoretic mobilities are now examined by comparing the corresponding surface charge for each possible ζ-potential with the charge for complete ionization of SDS at the decane−water interface. The surface charge corresponding to each ζ-potential is determined using eq 16 assuming $\psi = \zeta$, which is sufficient for discussing the degree of interfacial SDS counterion binding. To determine the SDS interfacial excess and charge using the Gibbs equation, we report decane−water interfacial tension as a function of bulk SDS concentration in Figure 6. The dashed curve is fitted by

$$\gamma(\ln [SDS]) = 27.36 - \frac{761.8}{(\ln [SDS])} - \frac{7126}{(\ln [SDS])^2} - \frac{14940}{(\ln [SDS])^3} \quad (21)$$

which is valid for the measured SDS concentrations between 0.001 and 5 mM, which are all below the SDS CMC of 8 mM. The SDS decane−water interfacial excess, Γ, is shown by the solid line in Figure 6 and is given by

$$\Gamma = -\frac{1}{N_A kT}\left(\frac{[NaNO_3]/[SDS] + 0.5}{[NaNO_3]/[SDS] + 1}\right)\left(\frac{d\gamma(\ln [SDS])}{d \ln [SDS]}\right)_{[NaNO_3]} \quad (22)$$

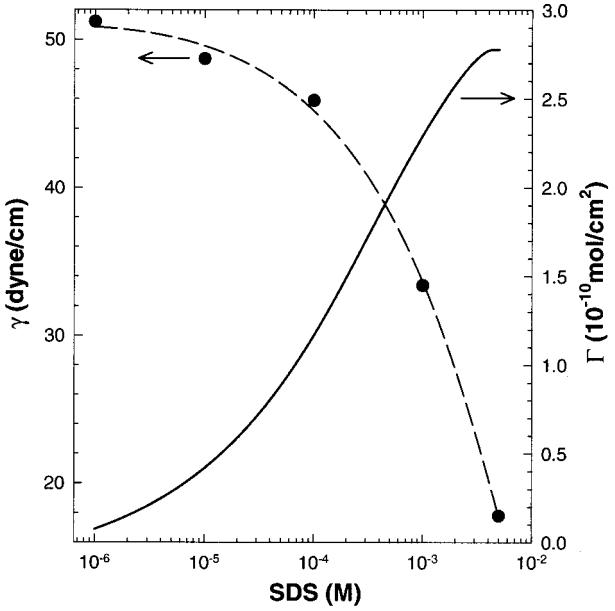

Figure 6. Interfacial tension data as a function of bulk SDS concentration from pendant droplet measurements at 298 K. The surface excess of surfactant with respect to the bulk SDS concentration is also shown as calculated from the Gibbs equation, eqs 17 and 22.

which is also limited to the measured SDS concentrations between 0.001 and 5 mM (all below the CMC = 8 mM), and a fixed $NaNO_3$ concentration of 1 mM. The correction in eq 22 for background $NaNO_3$ is not the most rigorous solution to the Gibbs equation,[26,30] but is appropriate here since interfacial tension has been shown to be unaffected by the NO_3^- anion in the literature.[31,32] The interfacial tension data, γ, and resulting interfacial excess, Γ, are in good agreement with literature values.[33−35] The fraction of interfacial SDS without bound counterion is interpreted as the ratio of the charge corresponding to the ζ-potential to the charge for completely ionized interfacial SDS. This fraction is defined by

$$f = \frac{\sigma_\zeta}{\sigma_\Gamma} = -\frac{2kT\epsilon_0\epsilon\kappa}{\Gamma e^2}\sinh\left[\frac{e\zeta}{2kT}\right] \qquad (23)$$

from eqs 16, 19, and 22, where f indicates the fraction ionized. Values of f are plotted in Figure 7 as a function of bulk SDS concentration for the data in row 2 of Table 2, which are the remaining ζ-potentials after consideration of the light scattering measurements of α. For reference in Figure 7, curves showing f as a function of constant ζ-potential are shown for $\zeta = -100$, -125, -150, -175, and -200 mV from eqs 21−23.

The results in Figure 7 allow us to select a single physically acceptable value of ζ-potential from the remaining possibilities for each SDS concentration. The most obvious ζ-potential choices which can be easily dismissed are those that correspond to $f > 100\%$, which are unphysical. For 0.01 mM SDS this additional information leaves $\zeta = -103$ mV as the only possible choice with $f =$

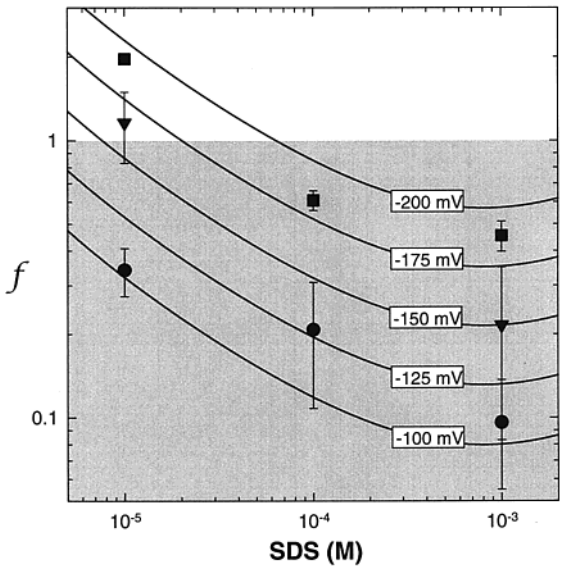

Figure 7. Fraction of ionization from eq 23. Values were calculated by comparing the surface charge density inferred from ζ-potentials in Table 3 using eq 16 and the surface charge density inferred from the surface excess assuming complete ionization using eq 19. For each SDS concentration, three ζ-potentials were possible from electrophoretic mobility data (after consideration of light scattering data): solid 1 (●), solid 2 (▼), and liquid 2 (■).

34%. After rejecting points with $f > 100\%$, the 0.1 and 1 mM SDS cases retain two and three possible ζ-potential choices. To further narrow the choices, it is useful to note that micelles typically have $f = 20\%$,[36,37] and previous SDS−oil−water interface studies have found $f = 10\%$.[33,34] With this information, the highest ζ-potential can be rejected for the 0.1 and 1 mM SDS cases, which have $f =$ 61% and $\%\sigma = 34\%$, respectively. For the 0.1 mM SDS case this leaves $\zeta = -128$ mV as the only possible choice with $f = 21\%$. Finally, the 1 mM SDS case has two possible ζ-potentials remaining, but $\zeta = -109$ mV with $f = 10\%$ appears to be the best option for several reasons: (1) the next higher ζ-potential with $f = 22\%$ is reasonable, but is high compared to literature values,[33,34] (2) the 0.01 and 0.1 mM SDS cases have less interfacial surfactant, but give the low ζ-potential rigid droplet solution suggesting the same solution for the 1 mM SDS case, and (3) the trend of decreasing percent ionization with increasing interfacial SDS suggests the ζ-potential with $f = 10\%$ for the 1 mM SDS as the appropriate choice. With the surface tension and light scattering data, it is possible to choose a single ζ-potential between -100 and -125 mV for each SDS concentration.

In the final analysis, the SDS/decane droplets all have ζ-potentials between -100 and -125 mV with no obvious dependence on bulk SDS concentrations between 0.01 and 1 mM. When the error associated with the mobility measurements, the unknown effect of counterion binding, and the changing droplet size with SDS concentration are considered, it is reasonable that the possible ζ-potential range is from -100 to -125 mV. Within experimental error, effects of a Stern layer or other subtleties do not appear necessary to describe these results beyond the basic mechanisms presented. The combination of light scattering and surface tension experiments permit the unambiguous conversion from electrophoretic mobility, μ, to ζ-potential. The surfactant-coated oil droplets were also

(30) Hall, D. G.; Pethica, B. A.; Shinoda, K. *Bull. Chem. Soc. Jpn.* **1975**, *48*, 324.
(31) Weissenborn, P. K.; Pugh, R. J. *Langmuir* **1995**, *11*, 1422.
(32) Weissenborn, P. K.; Pugh, R. J. *J. Colloid Interface Sci.* **1996**, *184*, 550.
(33) Haydon, D. A.; Taylor, F. H. *Philos. Trans. R. Soc. London* **1960**, *252*, 225.
(34) Kalinin, V. V.; Radke, C. J. *Colloids Surf., A* **1996**, *114*, 337.
(35) Staples, E.; Penfold, J.; Tucker, I. *J. Phys. Chem. B* **2000**, *104*, 606.
(36) Quina, F. H.; Toscana, V. G. *J. Phys. Chem.* **1977**, *81*, 1750.
(37) Drummond, C. J. *J. Colloid Interface Sci.* **1989**, *127*, 281.

shown to behave like solid particles in terms of their hydrodynamic mobility for all SDS concentrations studied here. In addition, we demonstrated that when SDS is used at concentrations below the CMC in the presence of decane, stable and nearly monodisperse oil droplets can be produced with sonication.

Acknowledgment. This work was supported by the Australian Research Council and the Particulate Fluids Processing Centre at the University of Melbourne. S.A.N. is a recipient of the Howard K. Worner Scholarship funded by BHP and Rio Tinto and an Australian Postgraduate Award. We are grateful to Dr. David Dunstan of the Department of Chemical Engineering/CRC for Bioproducts for providing use of the Malvern 4700 light scattering apparatus.

LA0103968